THE JOURNAL OF BIOLOGICAL CHEMISTRY VOL. 288, NO. 47, pp. 34276–34286, November 22, 2013

TROY Interacts with Rho Guanine Nucleotide Dissociation Inhibitor α (RhoGDIα) to Mediate Nogo-induced Inhibition of Neurite Outgrowth*

Received for publication, September 17, 2013, and in revised form, October 11, 2013 Published, JBC Papers in Press, October 15, 2013, DOI 10.1074/jbc.M113.519744

Yan Lu[1], **Xiujie Liu**[1], **Jianfeng Zhou, Aijun Huang, Jiazhen Zhou, and Cheng He**[2]

From the Institute of Neuroscience and Key Laboratory of Molecular Neurobiology, Ministry of Education, Neuroscience Research Centre of Changzheng Hospital, Second Military Medical University, Shanghai 200433, China

Background: TROY, together with the Nogo receptor, mediates Nogo-66 induced neurite outgrowth inhibition.
Results: TROY binds to RhoGDIα to activate RhoA and inhibit neurite outgrowth after Nogo-66 stimulation in cerebellar granule neurons.
Conclusion: TROY/RhoGDIα interaction transduces the inhibitory effects of Nogo-66 on neurite extension by activating RhoA.
Significance: TROY/RhoGDIα interaction plays a key role in RhoA activation and neurite outgrowth inhibition by Nogo-66.

TROY can functionally substitute p75 to comprise the Nogo receptor complex, which transduces the inhibitory signal of myelin-associated inhibitory factors on axon regeneration following CNS injury. The inhibition of neurite extension relies on TROY-dependent RhoA activation, but how TROY activates RhoA remains unclear. Here, we firstly identified Rho guanine nucleotide dissociation inhibitor α (RhoGDIα) as a binding partner of TROY using GST pull-down combined with two-dimensional gel electrophoresis and mass spectra analysis. The interaction was further confirmed by coimmunoprecipitation *in vitro* and *in vivo*. Deletion mutagenesis revealed that two regions of the TROY intracellular domain (amino acids 234–256 and 321–350) were essential for the interaction with RhoGDIα. Secondly, TROY and RhoGDIα were coexpressed in postnatal dorsal root ganglion neurons, cortex neurons, and cerebellar granule neurons (CGNs). Thirdly, TROY/RhoGDIα association was potentiated by Nogo-66 and was independent of p75/RhoGDIα interaction. Fourthly, TROY/RhoGDIα interaction was still able to activate RhoA when p75 was deficient. Furthermore, RhoA activation was decreased dramatically when TROY was knocked down in p75-deficient CGNs cells. Finally, RhoGDIα overexpression abolished RhoA activation and following neurite outgrowth inhibition by Nogo-66 in both wild-type and p75-deficient CGNs. These results showed that the association of RhoGDIα with TROY contributed to TROY-dependent RhoA activation and neurite outgrowth inhibition after Nogo-66 stimulation.

Myelin-associated inhibitory factors (MAIFs)[3] play a crucial role in the inhibition of axon regeneration and the limited functional recovery after CNS injury (1). Among five identified MAIFs, Nogo, myelin-associated glycoprotein, and oligodendrocyte myelin glycoprotein (OMgp) directly bind to the Nogo receptor complex, which can be composed of either Nogo receptor (NgR)·p75 neurotrophin receptor (p75)·LINGO-1 or NgR·TROY·LINGO-1 (2–4). The tripartite receptor complex then activates the small RhoA GTPase to induce growth cone collapse and exert inhibition of axonal regrowth as well as compensatory sprouting of remaining axons (5, 6).

TROY, an orphan receptor of tumor necrosis factor receptor (TNFR) superfamily member 19 (TNFRSF19), is more widely expressed in postnatal and adult neurons than p75. Different from p75, TROY exhibits a coordinated expression pattern with LINGO-1 and NgR. TROY, LINGO-1, and NgR all reach the highest expression at postnatal day 4 (P4) and decline slowly into adulthood (3). Furthermore, TROY shows a higher affinity for full-length NgR than p75 (3, 7). These results suggested that TROY might play a more important role than p75 in MAIFs-induced inhibition of neurite outgrowth in the postnatal CNS.

The mouse TROY is a single-pass type I transmembrane glycoprotein with 416 amino acids (Fig. 2*A*). The ectodomain (aa 30–170) of TROY contains cysteine-rich domains that are used by TNFR family members to bind to TNF-like ligands (8, 9). The hydrophobic stretch (aa 171–193) is assigned as the transmembrane domain of TROY. The intracellular domain (ICD) of TROY spans amino acids 194–416. The TROY ICD does not harbor the death domain discovered in p75 and some other TNFR family members (*e.g.* TNFRSF1A, TNFRSF6, and TNFRSF12) (9), although it has been found to be able to induce cell death (10, 11).

* This work was supported by National Key Basic Research Program Grant 2011CB504401, by National Natural Science Foundation of China Grants 31070922 and 31130024, and by Natural Science Foundation of Shanghai City Grant 13ZR1448500.

[1] Both authors contributed equally to this work.

[2] To whom correspondence should be addressed: Institute of Neuroscience and MOE Key Laboratory of Molecular Neurobiology, Neuroscience Research Center of Changzheng Hospital, Second Military Medical University, Shanghai 200433, China. Fax: 86-21-65492132; E-mail: chenghe@smmu.edu.cn.

[3] The abbreviations used are: MAIF, myelin-associated inhibitory factor; TNFR, tumor necrosis factor receptor; aa, amino acids; ICD, intracellular domain; RBD, Rhotekin binding domain; RhoGDIα, Rho GDP dissociation inhibitor α; P4, postnatal day 4; CGN, cerebellar granule neuron; TRITC, tetramethylrhodamine isothiocyanate; DRG, dorsal root ganglion; kd, knockdown.

As the transmembrane component of the NgR trimeric receptor complex, both TROY and p75 were able to mediate MAIF-induced inhibition of axonal regeneration through RhoA activation (7, 12). p75 has been found to facilitate the release of RhoA by competitive binding to the Rho guanine nucleotide dissociation inhibitor α (RhoGDIα) through its mastoparan-like α helix in the death domain (13). RhoGDIα is ubiquitously distributed across the postnatal CNS and can regulate RhoA activity by binding to and sequestering RhoA in the cytosol and protecting RhoA from formation of active RhoGTP (14). Unlike p75, TROY lacks the mastoparan-like α helix and the death domain in its intracellular region, which raises the question whether TROY can utilize RhoGDIα to achieve RhoA activation, thereby inhibiting neurite outgrowth. To date, the underlying mechanism that makes TROY activate RhoA remains elusive.

In this study, we identified RhoGDIα as a binding partner of TROY. The association of RhoGDIα with TROY was further confirmed *in vitro* and *in vivo*. Moreover, enhanced TROY/RhoGDIα interaction by Nogo-66 was independent of p75 and played an essential role in Nogo-66-induced RhoA activation and neurite outgrowth inhibition.

EXPERIMENTAL PROCEDURES

Animals—Sprague-Dawley rats and wild-type C57BL/6J mice were obtained from SIPPR/BK Experimental Animal (Shanghai, China). Mice with a functional-deficient mutation of p75 on the C57BL/6J background (15) was a gift from Dr. Zhen-Ge Luo (Institute of Neuroscience, Chinese Academy of Science, Shanghai, China). All procedures involving animal care and treatment were approved by the Animal Care and Use Committee of the Second Military Medical University (Shanghai, China) and performed according to the Guide for the Care and Use of Laboratory Animals (7th edition, National Institutes of Health, 1996).

Antibodies—Rabbit polyclonal anti-GST antibody (catalog no. G7781) and rabbit polyclonal anti-HA antibody (catalog no. H6908) were purchased from Sigma. Mouse monoclonal anti-His antibody (catalog no. AB 102) was from Tiangen (Beijing, China). Mouse monoclonal anti-Myc antibody (catalog no. 11667149001) was from Roche Applied Science. Rabbit polyclonal anti-RhoGDIα antibody (catalog 2564) and rabbit monoclonal anti-Myc antibody (catalog no. 2278) were from Cell Signaling Technology (Beverly, MA). Goat (catalog no. sc-13711) and rabbit (catalog no. sc-50320) polyclonal anti-TROY antibodies were purchased from Santa Cruz Biotechnology (Santa Cruz, CA). Mouse monoclonal anti-Tuj1 antibody (catalog no. G7121) was from Promega (Madison, WI).

Plasmids Construction and siRNA—pcDNA-Myc-RhoGDIα was provided by Dr. Lan Bao (Shanghai Institute of Biochemistry and Cell Biology, Chinese Academy of Science, Shanghai, China). The cDNAs for TROY-ICD and deletion mutants were amplified by PCR and subcloned into the pKH3 vector. Full-length RhoGDIα cDNA was inserted into the peGFP-N2 vector to generate GFP-RhoGDIα. cDNAs for TROY-ICD and Nogo-66 were subcloned into the pGEX-4T-1 vector (Amersham Biosciences) to generate GST fusion proteins. All constructs were fully sequenced before transformation or transfection. The siRNAs targeting mouse TROY (NM_013869) were designed and synthesized by Shanghai GeneChem (Shanghai, China). The siRNA sequences were as follows: 1#, 5-GGGAA-TGTTTCAGAA-TCTA-3; 2#, 5-GGTCTGTTTCCCGTTCC-AT-3; 3# 5-ACTGCAAGAGGCAGTTCAT-3; and 5-TTCTC-CGAACGTGTCACGT-3 as a scramble control.

Protein Purification and GST Pull-down Assay—GST and GST fusion proteins with TROY-ICD (aa 194–416) or Nogo-66 were expressed in *Escherichia coli* BL21 cells. All fusion proteins were precipitated with glutathione-Sepharose 4B beads (Amersham Biosciences) and eluted with 10 mM glutathione in 50 mM Tris (pH 8.0) according to the instructions of the manufacturer (Amersham Biosciences). A GST pull-down assay was performed as described previously (16). Briefly, equal amounts of immobilized GST fusion proteins were mixed and incubated for 3 h at 4 °C with brain lysates in GST binding buffer containing 40 mM HEPES, 50 mM sodium acetate, 200 mM NaCl, 2 mM EDTA, 5 mM dithiothreitol, 0.5% Nonidet P-40, and mixture protease inhibitors (Roche). Glutathione beads were washed three times in the same GST binding buffer. Then, the beads were eluted with SDS-PAGE sample buffer, and the supernatants were collected. For identification of possible TROY-ICD-binding proteins, the supernatants were subjected to two-dimensional SDS-PAGE/isoelectric focusing followed by MALDI-TOF/TOF mass spectra analysis. The supernatants were also applied to a denaturing 12% polyacrylamide gel, and Western blot analyses were conducted using anti-GST and anti-RhoGDIα antibodies to confirm the TROY/RhoGDIα interaction.

For the detection of direct TROY/RhoGDIα interaction, purified GST-TROY-ICD and His-RhoGDIα were used. Purified, bacterially expressed His-RhoGDIα was prepared using nickel-nitrilotriacetic acid-agarose (Qiagen, Chatsworth, CA) according to the protocols of the manufacturer. GST-TROY-ICD or GST was first incubated with glutathione-Sepharose 4B beads and then incubated with an equal amount of purified His-RhoGDIα in GST binding buffer. After washing, protein complexes were eluted from glutathione, separated on a 12% gel by SDS-PAGE, and followed by Western blot analysis.

Coimmunoprecipitation and Western Blot Analysis—HEK293T cell lysates, cerebellar granule neurons, and brain tissues homogenates from adult male Sprague-Dawley rats or 7-day-old C57/BL6J mice (P7) were prepared as described previously (17, 18). Briefly, the tissues and cells were lysed in solubilization buffer (25 mM HEPES-NaOH (pH 7.4), 125 mM potassium acetate, 5 mM $MgCl_2$, 0.32 M sucrose, 1% Triton X-100, and mixture protease inhibitors). Proteins solubilized from each homogenate were quantified using a BCA kit (Beyotime, Haimen, China). Equal amounts of protein were first incubated with primary antibodies for 3 h at 4 °C under mild agitation. Protein G-agarose beads (Roche) were then added for 3 h. After washing three times with solubilization buffer, the immunoprecipitated samples were boiled for 10 min in sample loading buffer and subjected to Western blot analysis.

For Western blot analysis, proteins were separated by electrophoresis in 12% SDS-PAGE and subsequently electrotransferred to a PVDF membrane (Millipore, Billerica, MA). After blocking, the membranes were incubated with primary anti-

bodies overnight at 4 °C under mild agitation. Horseradish peroxidase-conjugated secondary antibody (Kangcheng, Shanghai, China) was used. The blots were visualized by an ECL reaction system (Pierce). Densitometry analysis was performed by QuantityOne (Bio-Rad).

Cell Culture and Transfection—Cerebellar granule neuron (CGNs) cultures were prepared according to a procedure described previously (19) with minor modifications. Seven-day-old, wild-type C57BL/6J mice or p75-deficient mice were sacrificed by decapitation to get primary CGNs. After dissociation and filtering, cells were first cultured on poly-L-lysine-coated (0.1 mg/ml, Sigma), 6-well tissue culture plates or 8 × 8 mm coverslips and maintained in DMEM/F12 with 10% fetal bovine serum (Invitrogen). Neurobasal-A medium completed with 2% B27 supplement (Invitrogen), 1% N2 supplement, 20 mM Gluta MAX, and 100 units/ml penicillin and streptomycin (Invitrogen,) was used 3 h later. Cells were kept at 37 °C in a humidified atmosphere of 5% CO_2 and 95% air. After 24-hour incubation, the CGNs were harvested for coimmunoprecipitation or Western blot analysis.

For transfection of DNA constructs, CGNs were subjected to electrotransfection (O-05 program, Amaxa Biosystems, Köln, Germany) right after dissection and according to the instructions of the manufacturer. The cells were plated directly on coverslips precoated with 10 μg/ml mouse laminin (Invitrogen) in 10% FBS/DMEM. The culture medium was replaced with fresh medium 3 h after transfection.

Immunocytochemistry and Immunohistochemistry—Cultured cells were gently rinsed with PBS, fixed with 4% paraformaldehyde in 0.1 M phosphate buffer (pH 7.4) for 20 min at room temperature, and permeabilized with 0.3% Triton X-100. The fixed cells were incubated with primary antibodies overnight at 4 °C and then stained with FITC- or TRITC-conjugated secondary antibodies (Jackson ImmunoResearch Laboratories and Vector Laboratories).

For immunohistochemistry, animals were anesthetized and perfused transcardially with 4% paraformaldehyde in 0.1 M phosphate buffer (pH 7.2) (20). Brains were removed from the cranial vaults, post-fixed for 2 h in the same fixative, and then cryopreserved overnight in 20% sucrose in 0.1 M phosphate buffer at 4 °C. Frozen sections were cut at a thickness of 14 μm and incubated in blocking buffer containing 5% BSA and 0.5% Triton X-100 for 20 min. After blocking, the brain sections were incubated overnight at room temperature with primary antibodies diluted in the same blocking buffer. After rinsing in PBS, sections were incubated with FITC- or TRITC-conjugated anti-rabbit, anti-mouse, or anti-goat IgG antibodies. Images were obtained using a Nikon fluorescent microscope or a Leica SP5 confocal microscope.

RhoA Activation Analysis—RhoA activity in cell lysates was analyzed using a Rho activation assay kit (Millipore) according to the instructions of the manufacturer and our previous report (21). Briefly, CGN cultures were stimulated by GST or GST-Nogo-66 (100 nM) (2) for specified time periods before being lysed in 250 μl of supplied lysis buffer containing mixture protease inhibitors. About 20 μl of each lysate was used for protein quantification and Western blot analysis of total RhoA. For detection of the active RhoA (GTP-bound RhoA), equal amounts of protein from each sample were incubated with Rhotekin binding domain (RBD) affinity agarose beads for 45 min at 4 °C. After centrifugation (10 s, 14,000 × *g*, 4 °C), pellet beads were washed three times in the wash buffer. Bound proteins were collected and examined by Western blot analysis. The amount of GTP-bound RhoA was normalized to the total amount of RhoA in cell lysates as described previously (22, 23) and then normalized to values at time 0 min. Statistical analysis was performed for data from three independent experiments. Data were shown as mean ± S.D.

Neurite Outgrowth Assay—A neurite outgrowth assay was performed as described previously (24, 25). After GFP-RhoGDIα or control GFP-N2 vector transfection, dissociated primary CGNs were plated onto immobilized substrate (GST or GST-Nogo-66 (50 ng/cm^2) (2). Cells were cultured for 24 h before fixation and staining. Cells were observed under a fluorescent microscope (Nikon). Neurite lengths were measured using ImageJ software. For each GFP-positive neuron, the length of the longest neurite was measured. The averaged neurite lengths of each group were normalized to that of wild-type CGNs with neither Nogo-66 treatment nor RhoGDIα overexpression. Three independent experiments, at least 150 neurons/condition from duplicate wells, were performed. The data were analyzed by one-way analysis of variance with post hoc Bonferroni (homogeneity of variances assumed) or Games-Howell (homogeneity of variances not assumed) comparisons. All values were expressed as mean ± S.D.

RESULTS

RhoGDIα Interacts with TROY in Vitro and in Vivo—Although TROY acts as a coreceptor to form a tripartite complex with NgR·LINGO-1 and activates RhoA to exert axon regrowth inhibition (2, 3), the possible mechanism by which TROY activates RhoA is scarcely reported. We proposed to gain an insight into the TROY signaling pathway through searching binding partners of the TROY-ICD. GST-TROY-ICD fusion protein was expressed in *E. coli* BL21 cells, extracted, and purified. The purified GST-TROY-ICD recombinant protein was then incubated with rat brain lysates to pull down the binding candidates. GST protein was used as the control for GST-TROY-ICD. The bound samples were subjected to two-dimensional SDS-PAGE/isoelectric focusing with MALDI-TOF/TOF mass spectra analysis. Using the Mascot program (Matrix Science, London, UK), we identified RhoGDIα as a candidate with the following indicators: Mascot score, 95; molecular weight, 23393; calculated pI, 5.12; and percent sequence coverage, 32%.

The association of RhoGDIα with the TROY-ICD was further confirmed by GST precipitation assay with rat brain lysates. As shown in Fig. 1*A*, endogenous RhoGDIα could be precipitated by GST-TROY-ICD but not by GST. We next checked the direct interaction between TROY and RhoGDIα using an *in vitro* GST pull-down assay with purified His-RhoGDIα and GST-TROY-ICD. Consistent with the above results, we found that GST-TROY-ICD, but not GST, could interact with His-RhoGDI α (Fig. 1*B*).

To further investigate whether TROY-ICD and RhoGDIα could form a complex *in vitro* and *in vivo*, a reciprocal coimmunoprecipitation assay was performed. In HEK293T cells expressing

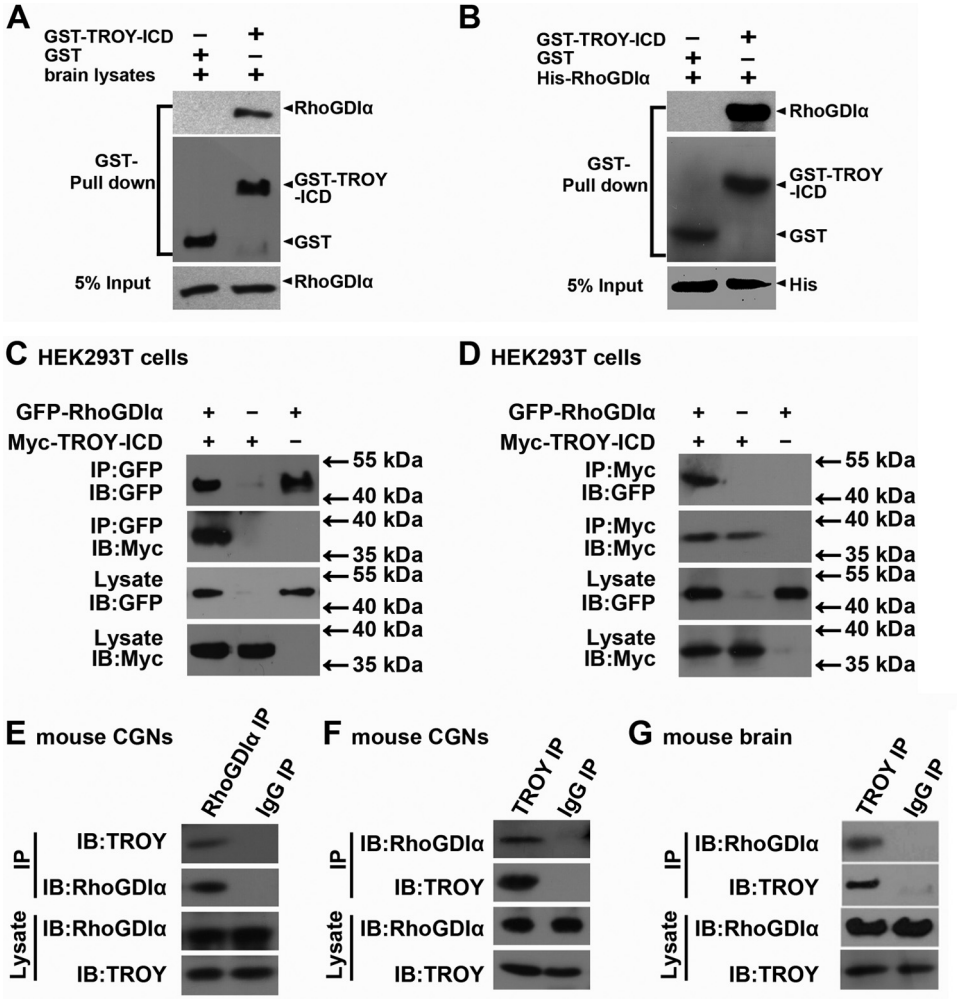

FIGURE 1. **TROY interacts with RhoGDIα**. *A* and *B*, GST pull-down assay. Purified GST-TROY-ICD was incubated with lysates from adult rat brain (*A*) and purified His-RhoGDIα (*B*). The bound samples were analyzed by immunoblot analysis with anti-RhoGDIα, anti-GST, and anti-His. The 5% input of GST-fusion proteins is shown at the bottom. *C* and *D*, coimmunoprecipitation using recombinant proteins. Lysates of HEK293T cells transfected with GFP-RhoGDIα and Myc-TROY-ICD were first immunoprecipitated (*IP*) with anti-GFP (*C*) or anti-Myc (*D*) followed by immunoblot (*IB*) analysis with anti-Myc or anti-GFP, respectively. *E* and *F*, coimmunoprecipitation *in vitro* using endogenous proteins. Lysates from C57BL/6J (P7) CGNs were immunoprecipitated with anti-RhoGDIα or anti-TROY antibodies, followed by immunoblot analysis with anti-TROY and anti-RhoGDIα antibodies, respectively. Normal mouse or goat IgG (*IgG IP*) was used as the control. *G*, coimmunoprecipitation *in vivo* using endogenous proteins. 500 μg of protein from homogenates of adult mouse brain was subjected to immunoprecipitation with anti-TROY antibody. Normal goat IgG (*IgG*) was used as the control. Resulting immunocomplexes were probed with anti-mouse RhoGDIα antibody. 10% of lysates were loaded as input (*bottom panel*).

both GFP-tagged RhoGDIα and Myc-tagged TROY-ICD (Fig. 1, *C* and *D*), GFP-RhoGDIα could specifically immunoprecipitate with Myc-TROY-ICD and vice versa. Moreover, in lysates of cultured mouse CGNs (Fig. 1, *E* and *F*) and mouse whole brain (*G*), endogenous TROY and RhoGDIα were immunoprecipitated with each other. These data supported the interaction of TROY with RhoGDIα *in vitro* and *in vivo*.

Amino Acids 234–256 and 321–350 of TROY Are Required for RhoGDIα Binding—Because TROY-ICD does not contain the death domain and the mastoparan-like α helix that p75 uses to bind to RhoGDIα (Fig. 2*A*), we next mapped the region responsible for TROY/RhoGDIα interaction by deletion mutagenesis. A series of C- and N-terminal truncation mutants of TROY-ICD tagged with HA were constructed and named mutant 1–8 (Fig. 2*B*, *M1–8*). These mutants were separately cotransfected into HEK293T cells with GFP-RhoGDIα. The transfected cells were lysed 48 h later and subjected to Western blot analysis using anti-HA or anti-GFP antibody. All of the TROY-ICD mutants and RhoGDIα constructs were detected at the predicted molecular mass (Fig. 2*C*, *bottom panel*). The lysates were then subjected to coimmunoprecipitation followed by immunoblot analysis with the corresponding antibodies. When an anti-GFP antibody was used to immunoprecipitate with the cell lysates, HA-tagged M1 (aa 194–390), M2 (aa 194–371), M3 (aa 194–350), and M6 (aa 234–416) were detected in the precipitates, whereas M4 (aa 194–321), M5 (aa 194–285), M7 (aa 256–416), and M8 (aa 276–416) were not detected (Fig. 2*C*). When cotransfected cell lysates were subjected to immunoprecipitation with the anti-HA antibody, GFP-tagged RhoGDIα cotransfected with M1, M2, M3, and M6, but not M4, M5, M7, or M8, were detected in the precipitates (Fig. 2*D*). We are inclined to conclude that two regions of TROY-ICD (aa 234–256 and 321–350) are indispensable for RhoGDIα association, although it is possible that the largest N-terminal and C-terminal deletions present in M7/M8 and M4/M5, respectively, may affect interaction through misfolding.

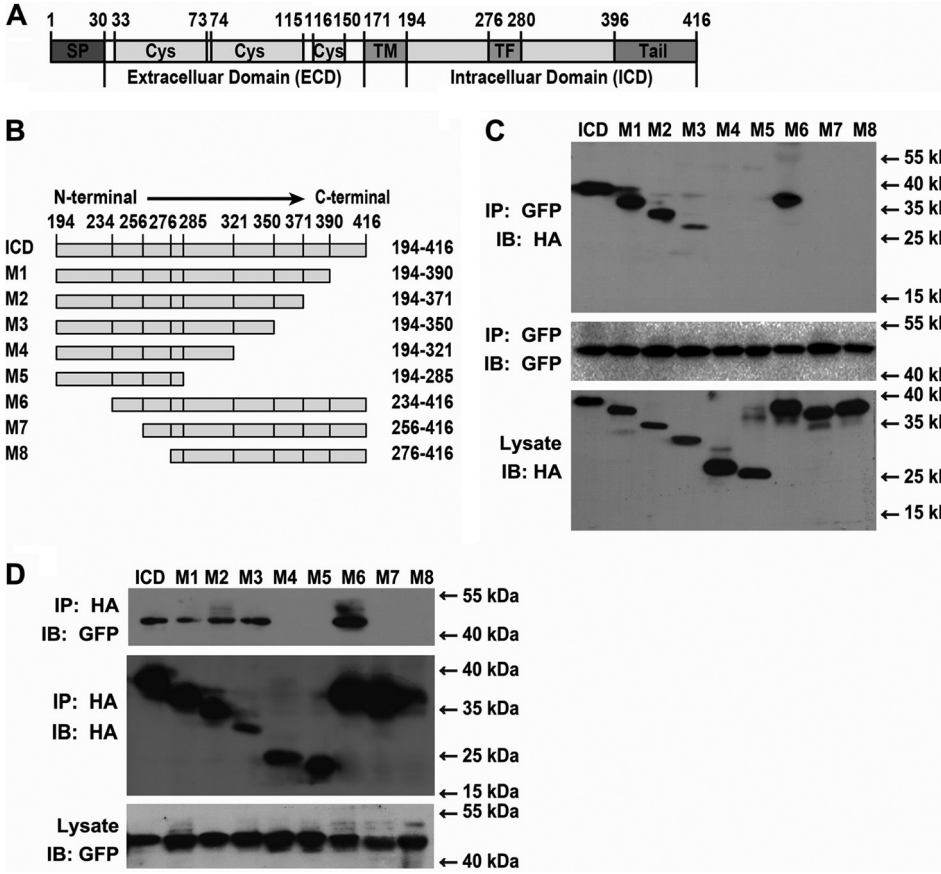

FIGURE 2. **Mapping the region of TROY for RhoGDIα interaction by deletion mutagenesis.** *A*, schematic representation of mouse TROY. *SP*, signal peptide; *Cys*, cysteine-rich motifs; *TM*, transmembrane domain; *TF*, TRAF2-binding domain; *Tail*, cytoplasmic tail. The numbers denote the starting numbers of amino acids for each domain. *B*, schematic of TROY-ICD deletion constructs. The numbers on the right denote the starting and ending numbers of the amino acids of the mutants. *C* and *D*, HEK293T cells were transfected with each of the HA-tagged mutant constructs plus GFP-tagged RhoGDIα, respectively. Cell lysates were first immunoprecipitated (*IP*) with anti-GFP (*C*) or anti-HA (*D*) antibodies, followed by immunoblot analyses (*IB*) with anti-HA or anti-GFP antibodies.

TROY Is Colocalized with RhoGDIα in Postnatal Neurons—As colocalization was the premise of functional interaction, we next examined whether TROY and RhoGDIα were colocalized in postnatal neurons. Double immunofluorescent staining revealed that both TROY and RhoGDIα were strongly expressed in primary CGNs, dorsal root ganglion (DRG) neurons, and cortex neurons (Fig. 3, *A–C*). Furthermore, immunohistochemistry showed that TROY and RhoGDIα were coexpressed in most DRG neurons and were broadly codistributed in the cerebellum and cerebral cortex neurons (Fig. 3, *D–F*). These results support the coexpression pattern of TROY and RhoGDIα in postnatal neurons in these regions.

TROY/RhoGDIα Interaction Is Enhanced by Nogo-66 Stimulation—To resist the possibility that TROY/RhoGDIα interaction was incidental or not associated with MAIF signaling, we examined the influence of Nogo-66 treatment on TROY/RhoGDIα interaction in cultured CGNs. After GST or GST-Nogo-66 (100 nM) treatment for 30 min, the CGNs were lysed and subjected to immunoprecipitation to detect the association of TROY with RhoGDIα. As shown in Fig. 4, *A* and *B*, GST-Nogo-66 but not GST treatment significantly enhanced TROY/RhoGDIα association. p75 has been reported to be coexpressed with TROY and could associate with RhoGDIα in CGNs (26). To exclude the possible influences of p75, we repeated the experiment in cultured p75-deficient ($p75^{-/-}$) CGNs. As shown in Fig. 4, *C* and *D*, the significant increase of TROY/RhoGDIα association by GST-Nogo-66 was still detected when p75 was deficient. Taken together, these results demonstrated that the association of TROY with RhoGDIα was potentiated by Nogo-66 stimulation and was independent of p75.

RhoA Is Activated by Nogo-66 Stimulation in both Wild-type and $p75^{-/-}$ CGNs—RhoA activation is a pivotal signaling event during MAIF-induced neurite outgrowth inhibition (27, 28). We next tested whether RhoGDIα was involved in TROY-mediated RhoA activation upon Nogo-66 stimulation. Cultured CGNs were treated with Nogo-66 (100 nM) for several specified time periods. Afterward, RhoA activity was detected using a GST-fused Rho-binding domain of Rhotekin that could precipitate GTP-bound active RhoA (21). As shown in Fig. 5, *A* and *B*, Nogo-66 (100 nM) rapidly activated RhoA in about 15 min in wild-type CGNs. The increased RhoA activities were also detected when Nogo-66 was present for 30 and 60 min (Fig. 5, *A* and *B*).

We also determined the role of TROY in RhoA activation using $p75^{-/-}$ or TROY knockdown (TROY-kd) CGNs. A significant increase of RhoA activity was observed 30 and 60 min, but not 15 min, after Nogo-66 stimulation in these CGNs (Fig. 5, *C–F*). However, the Nogo-induced RhoA activation was reduced in either $p75^{-/-}$ or TROY-kd CGNs compared with

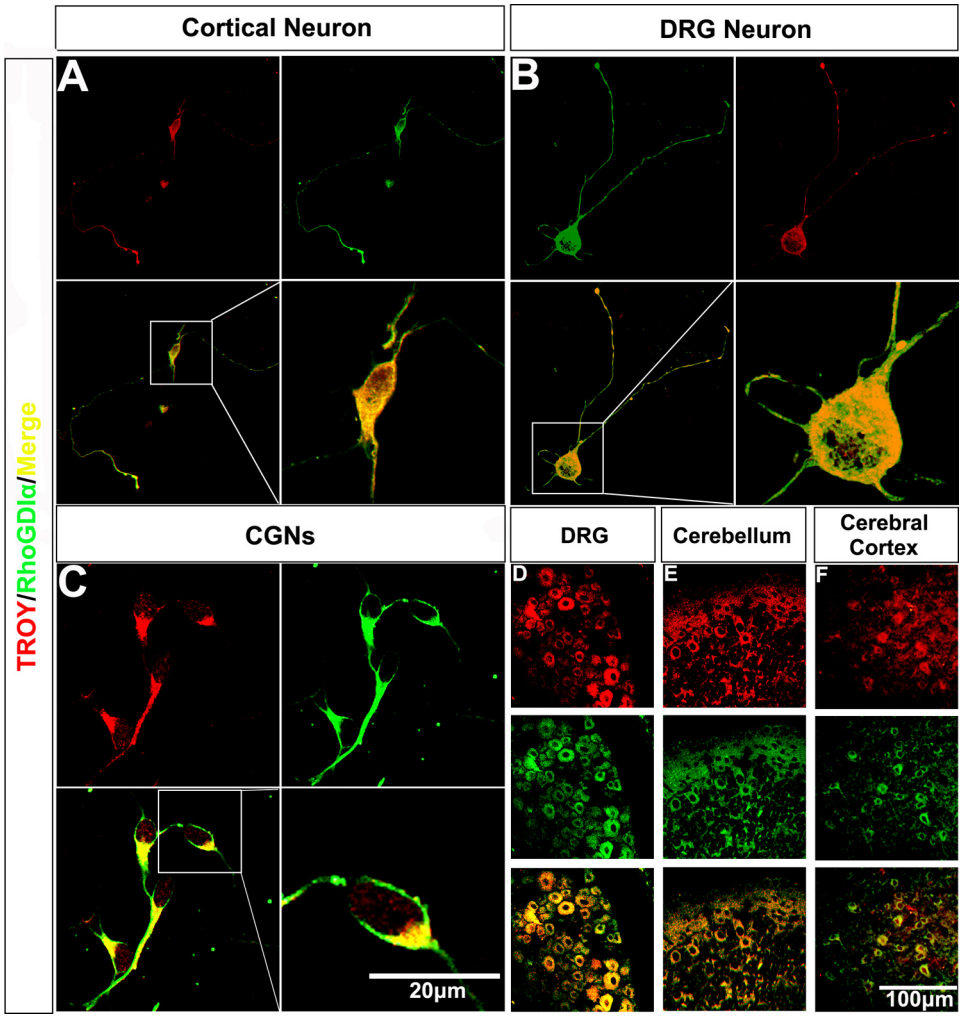

FIGURE 3. **TROY and RhoGDIα are colocalized in postnatal neurons.** Primary cultured C57BL/6J mouse (P7) Cortical neurons (*A*), DRG neurons (*B*), and CGNs (*C*) were double-stained with anti-TROY (*red*) and anti-RhoGDIα (*green*). The overlaid images (*yellow*) indicate that RhoGDIα and TROY were expressed and colocalized. *Scale bar* = 20 μm. *D–F*, adult mouse DRG, cerebral cortex, and cerebellum cryosections were double-stained with anti-TROY (*red*) and anti-RhoGDIα (*green*). The overlaid images (*yellow*) indicate that TROY was widely codistributed with RhoGDIα in these regions. The images were obtained using a confocal microscope. *Scale bar* = 100 μm.

wild-type CGNs. Furthermore, RhoA activation was dramatically decreased when TROY was knocked down in $p75^{-/-}$ CGNs cells (Fig. 5, *G* and *H*). These results suggested that either p75 or TROY was able to mediate Nogo-66 induced RhoA activation in CGNs.

RhoGDIα Overexpression Eliminates Neurite Outgrowth Inhibition and RhoA Activation Induced by Nogo-66—Because Nogo-66 enhanced TROY/RhoGDIα interaction, the increased RhoA activity and following neurite outgrowth inhibition by Nogo-66 might be attributed to the dissociated RhoA from RhoGDIα, which was recruited to TROY. We supposed that RhoGDIα overexpression, which attenuated TROY/RhoGDIα-induced RhoA activation, could abolish the inhibitory effect of Nogo-66 on neurite outgrowth. To test this hypothesis, GFP-RhoGDIα was overexpressed in the wild-type and $p75^{-/-}$ CGNs. GFP was used as the control. The primary CGNs were subjected to Nogo-66 treatment for 24 h, and the neurite lengths were measured. As shown in Fig. 6, *A* and *B*, Nogo-66 inhibited neurite extension in both wild-type and $p75^{-/-}$ neurons. Moreover, less of an inhibitory effect was observed in $p75^{-/-}$ CGNs compared with that in wild-type CGNs. RhoGDIα overexpression had no significant effect on neurite length of either type of neurons when Nogo-66 was not administered. However, RhoGDIα overexpression eliminated the inhibitory effects of Nogo-66 on neurite outgrowth either in wild-type neurons, where both TROY and p75 exist, or in $p75^{-/-}$ neurons (Fig. 6, *A* and *B*).

We also examined RhoA activity of CGNs after 24-hour Nogo-66 treatment. As shown in Fig. 6, *C* and *D*, a significant increase of RhoA activity was observed in wild-type, $p75^{-/-}$, and TROY-kd CGNs after Nogo-66 stimulation. Compared with the wild-type CGNs, RhoA activity was only slightly decreased in either $p75^{-/-}$ or TROY-kd CGNs when treated with Nogo-66 for 24 h, which was accompanied by the observation that the absence of p75 caused less of an inhibitory effect on neurite outgrowth upon Nogo-66 treatment. Meanwhile, RhoA activation was significantly reduced when TROY was knocked down in p75-deficient CGNs cells. When RhoGDIα was overexpressed, significantly diminished RhoA activation was observed in wild-type, $p75^{-/-}$, TROY-kd, and $p75^{-/-}$/

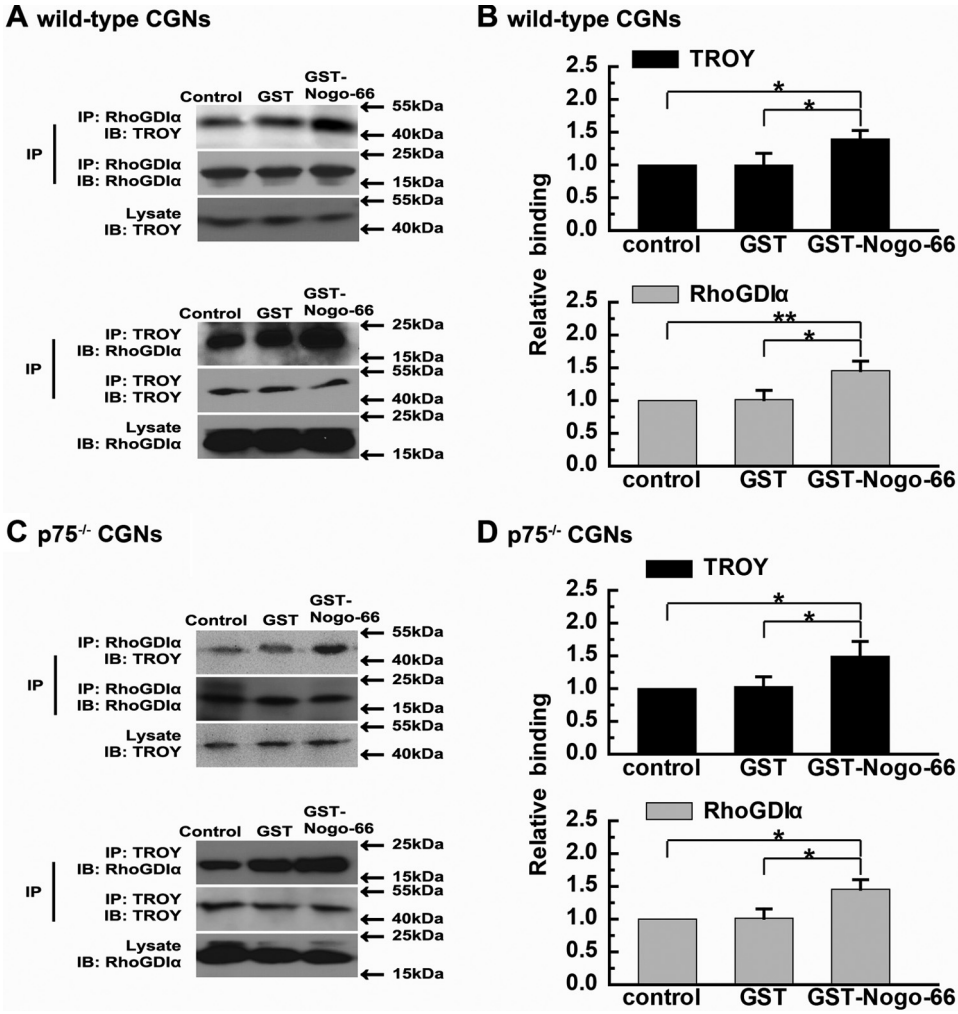

FIGURE 4. **TROY/RhoGDIα interaction is enhanced by Nogo-66 in a p75-independent way.** *A* and *B*, blot images (*A*) and histograms (*B*) showing enhanced RhoGDIα/TROY interaction by Nogo-66 stimulation in wild-type CGNs. Primary cultured mouse P7 CGNs were treated with 100 nM GST-Nogo-66 or GST or vehicle control for 30 min. Cell lysates were immunoprecipitated (*IP*) with anti-RhoGDIα or anti-TROY and subsequently immunoblotted (*IB*) with anti-TROY or RhoGDIα. The inputs (*bottom panels*) represent 5% of the lysates for immunoprecipitation. Data were normalized to blot densities from the control group. Data are expressed as mean ± S.D. of three independent experiments. *, $p < 0.05$; **, $p < 0.01$. *C* and *D*, representative blot images and histograms showing enhanced RhoGDIα/TROY interaction by Nogo-66 stimulation in p75-deficient $p75^{-/-}$ CGNs. *, $p < 0.05$.

TROY-kd CGNs, and RhoA activation by Nogo was decreased significantly in $p75^{-/-}$/TROY-kd CGNs cells. Taken together, these results demonstrated that TROY/RhoGDIα interaction was involved in TROY-mediated RhoA activation and that neurite outgrowth inhibition induced by Nogo-66.

DISCUSSION

Both TROY and p75 can form a receptor complex with NgR·LINGO-1 and transduce the signal of myelin inhibitors (2, 3). It has been reported that p75 utilized the mastoparan-like α helix, which is sited in the death domain, to bind to RhoGDIα and displaced RhoA from inactivation (13). However, neither death the domain nor mastoparan-like α helix was found in the intracellular region of TROY (9, 29), which suggested that TROY might not be able to directly bind to RhoGDIα to activate RhoA. Unexpectedly, in this study, we identified RhoGDIα as a binding partner of TROY (Fig. 1). In addition, we found that two intracellular regions of TROY (aa 234–256 and 321–350) played an essential role in the interaction with RhoGDIα (Fig. 2). Furthermore, the interaction between TROY and RhoGDIα was similarly enhanced in both wild-type and $p75^{-/-}$ CGNs following Nogo-66 stimulation, which suggested that the interaction between TROY and RhoGDIα was independent of the p75 receptor (Fig. 4). This indicated that the intracellular domain of TROY, which was distinct from that of p75, could also transduce the downstream signals of Nogo-66 via binding to RhoGDIα.

Rho GTPases such as RhoA, RhoC, and Rac1 have been reported to exert essential functions in regulating various biological episodes such as cell migration, proliferation, neuronal process guidance, and so forth (30–32). In particular, RhoA was considered as a negative regulator of neurite extension (30–32). RhoA activity was tightly controlled by the RhoGTPase cycle. Among the regulatory proteins involved in the RhoGTPase cycle, RhoGDIα was a limiting factor for RhoA activation (33, 34). In this study, we demonstrated that RhoA activation by Nogo-66 was accompanied by enhanced TROY/RhoGDIα interaction (Fig. 4). Furthermore, RhoGDIα overexpression

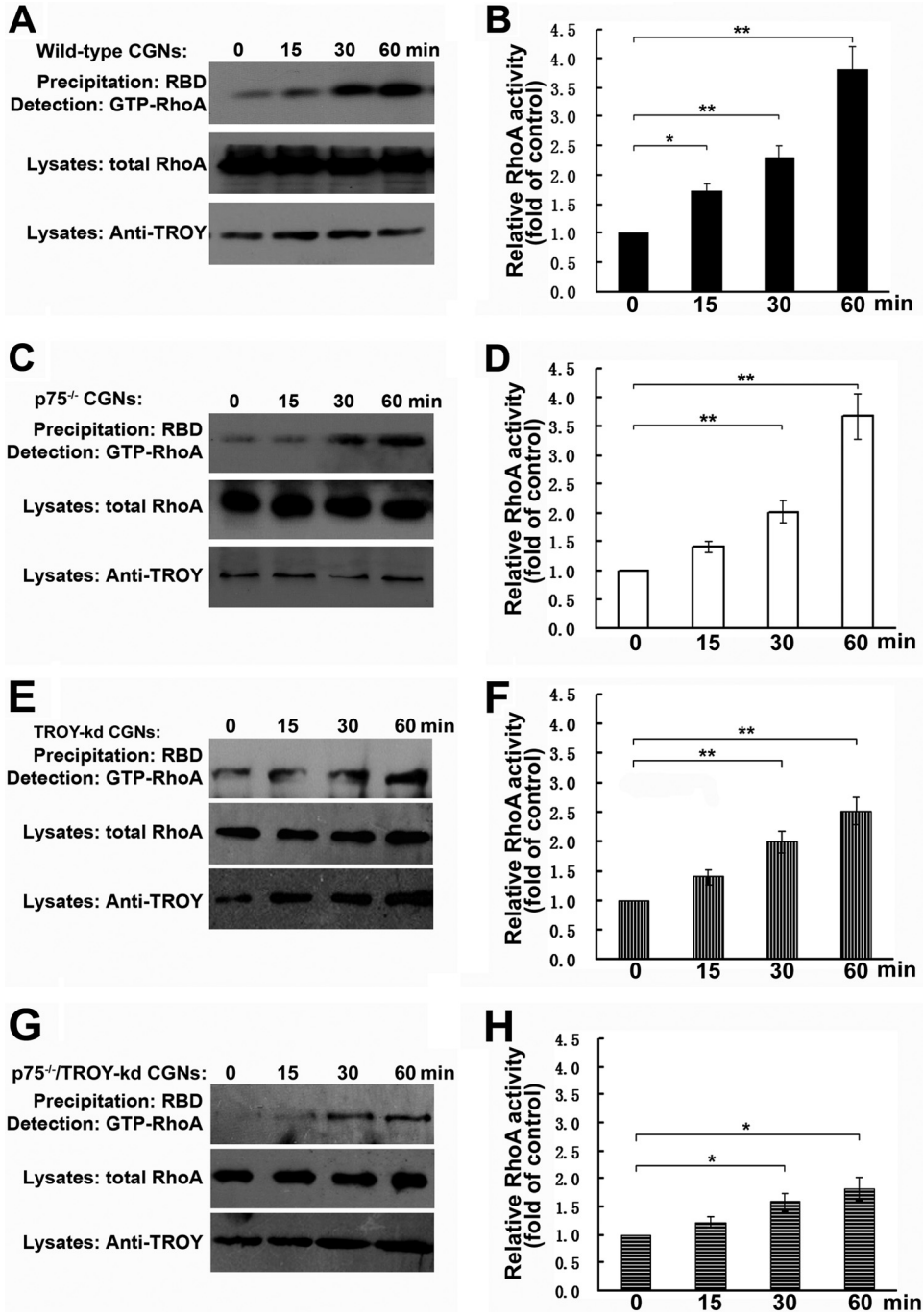

FIGURE 5. **RhoA is activated by Nogo-66 through TROY/RhoGDIα interaction.** *A* and *B*, representative blots (*A*) and histograms (*B*) showing RhoA activation by Nogo-66 in WT CGNs. RhoA activity was indicated by the amount of RBD-bound RhoA (*GTP-RhoA*) first normalized to that of total RhoA in cell lysates and then normalized to values at time 0. Data are expressed as mean ± S.D. of three independent experiments. *, $p < 0.05$; **, $p < 0.01$. *C* and *D*, representative blots (*C*) and histograms (*D*) showing RhoA activation by Nogo-66 in $p75^{-/-}$ CGNs. **, $p < 0.01$. *E* and *F*, representative blots (*E*) and histograms (*F*) showing RhoA activation by Nogo-66 in TROY-kd CGNs. **, $p < 0.01$. *G* and *H*, representative blots (*G*) and histograms (*H*) showing RhoA activation by Nogo-66 in $p75^{-/-}$/TROY-kd CGNs. *, $p < 0.05$.

diminished RhoA activation in wild-type, $p75^{-/-}$, TROY-kd, and $p75^{-/-}$/TROY-kd CGNs, whereas RhoA activation by Nogo was decreased significantly decreased in $p75^{-/-}$/TROY-kd CGNs cells (Fig. 6, *C* and *D*). These results suggested that TROY/RhoGDIα association was crucial for TROY-mediated RhoA activation induced by Nogo-66.

Consistent with reports of other groups that increased RhoA activity could be detected from 10 min to 24 h in MAIF-treated neurons (35, 36), RhoA was activated continuously (24 h) in both wild-type and $p75^{-/-}$ CGNs after Nogo-66 treatment in our study (Fig. 5). We found that Nogo-66-induced RhoA activation was only moderately reduced in $p75^{-/-}$ CGNs (Fig. 5, *C* and *D*). In addition, the RhoA activity was also slightly decreased in TROY-kd cells (Fig. 5, *E* and *F*). However, RhoA activation was decreased dramatically in $p75^{-/-}$/TROY-kd CGNs (Fig. 5, *G* and *H*). As both TROY and p75 were expressed

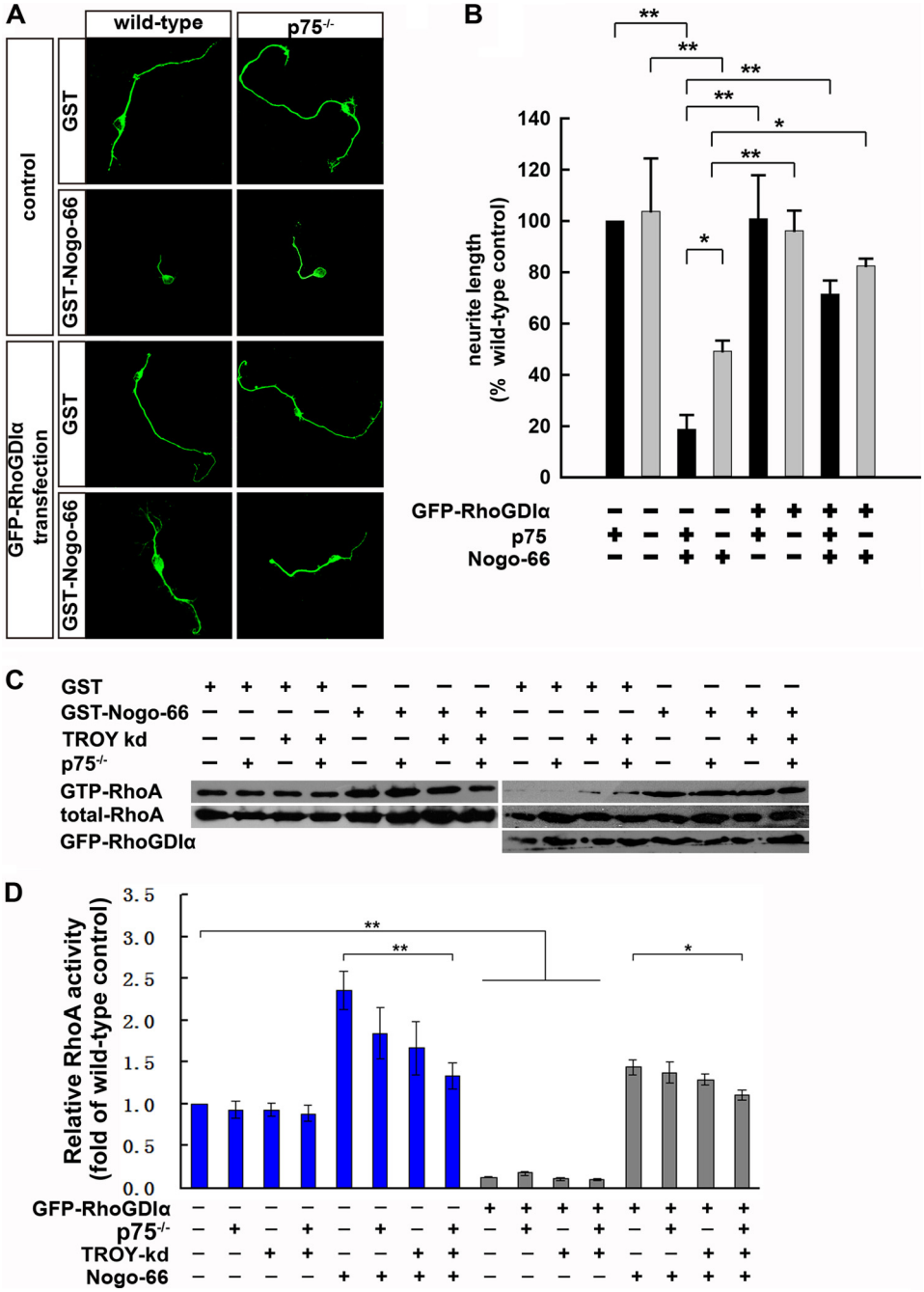

FIGURE 6. **RhoGDIα overexpression eliminates neurite outgrowth inhibition and RhoA activation induced by Nogo-66.** *A* and *B*, images (*A*) and histograms (*B*) showing neurite outgrowth in wild-type and $p75^{-/-}$ CGNs. CGNs transfected with GFP or GFP-RhoGDIα were grown on either GST-Nogo-66 or GST (control)-coated slides. After 24 h, neurons were subjected to immunostaining and visualized using confocal microscopy. *Scale bar* = 20 μm. Neurite length was quantified by measuring the lengths of the longest individual neurites from at least 150 neurons. Data were expressed as mean ± S.D. *, $p < 0.05$; **, $p < 0.01$. *C* and *D*, immunoblot analyses (*C*) and histograms (*D*) showing RhoA activities after 24-hour Nogo-66 treatment in wild-type, $p75^{-/-}$, TROY-kd, and $p75^{-/-}$/TROY-kd CGNs. RhoA activity is indicated by the amount of GTP-RhoA normalized to that of total RhoA in cell lysates and normalized to values of wild-type CGNs without Nogo-66 treatment at time 0. Data are expressed as mean ± S.D. of three independent experiments. *, $p < 0.05$; **, $p < 0.01$.

in CGNs, they may play complementary roles in mediating RhoA activation induced by Nogo-66. Nevertheless, these results suggested a crucial role of TROY in mediating Nogo-66 induced RhoA activation.

In the adult mouse, p75 expression was limited to a small subpopulations of spinal cord-ascending sensory neurons, DRG neurons, and retinal ganglion neurons and was undetectable in the cerebral cortex, cerebellum, and most retinal ganglion neurons (35, 37), where neurons were also MAIF-responsive (2). In contrast, TROY was widely expressed across most of these regions. The higher expression levels of TROY were detected at postnatal day 23 and in adulthood compared with p75 (2–4). Consistent with previous reports (2, 3, 38), our study showed that TROY was expressed broadly and confined to the RhoGDIα-expressing neurons in the adult cerebral cortex, cerebellum, and DRG (Fig. 3). These results suggest a possibly wider role of TROY/RhoGDIα interaction in the context of the MAIF-NgR network.

In addition to the more widely and coordinated distribution of TROY with NgR and LINGO-1, TROY bound to NgR with a near 8-fold higher affinity than p75 (2, 7). Our results showed that TROY interacted with RhoGDIα in a p75-independent way (Fig. 4). Furthermore, the NgR·TROY·LINGO-1 complex still showed equal efficiency in activating RhoA compared with the NgR·p75·LINGO-1 complex when a high concentration of Nogo-66 (100 nM) was administered (2). These results suggested that TROY was superior to p75 in mediating Nogo-66-induced RhoA activation and following neurite extension inhibition via binding to RhoGDIα.

In support of our notion, Shao *et al.* (3) reported that TROY-deficient CGNs were resistant to low-dose (500 ng and 1 μg) Nogo-66 stimulation. The results suggested that low-dose Nogo-66 preferred to utilize the TROY/RhoGDIα interaction rather than the p75/RhoGDIα interaction to transduce the inhibitory signal. When high-dose Nogo-66 was administered, both TROY and p75 seemed to contribute to neurite outgrowth inhibition, as less neurite outgrowth inhibition induced by Nogo-66 was observed in $p75^{-/-}$ neurons (Fig. 6, *A* and *B*) and TROY-deficient neurons compared with that in wild-type neurons (2, 3). However, a truncated TROY lacking its intracellular domain but not a truncated p75 protein lacking the intracellular domain fully reversed the inhibitions by Nogo-66 in both wild-type and p75-deficent neurons (2, 3, 24). The evidence that targeting TROY but not p75 could rescue Nogo-66/NgR signaling suggests that TROY might play more important roles in Nogo-66 induced axonal regeneration inhibition in postnatal CNS.

TROY was highly expressed in astrocytes and microglia that did not have NgR or LINGO-1 protein expression (39, 40). Meanwhile, RhoGDIα was ubiquitously expressed in these glial cells (41, 42) and was involved in the regulation of RhoA, RhoC, and Rac1 activity (43). These findings suggest that the function of TROY/RhoGDIα interaction in the nervous system might not be limited to neurite outgrowth regulation. TROY expression has been found to be elevated in both human glioma cells and infiltrating microglia (44, 45). The increased TROY expression was strongly inversely related with the life span of patients (44). Meanwhile, RhoGDIα was found to be down-regulated in glioma cells (41, 46). Furthermore, the increased TROY expression and decreased RhoGDIα expression were accompanied with reduced RhoA activation and increased Rac1 activation in glioma cells (44, 47–49). It would be interesting to further examine the role of TROY/RhoGDIα interaction in glial tumor invasion and progression.

Acknowledgments—We thank Dr. Xu Zhang (Institute of Neuroscience, Chinese Academy of Science, Shanghai, China) for technical support in immunohistochemistry studies on DRG neurons.

REFERENCES

1. Filbin, M. T. (2003) Myelin-associated inhibitors of axonal regeneration in the adult mammalian CNS. *Nat. Rev. Neurosci.* **4**, 703–713
2. Park, J. B., Yiu, G., Kaneko, S., Wang, J., Chang, J., He, X. L., Garcia, K. C., and He, Z. (2005) A TNF receptor family member, TROY, is a coreceptor with Nogo receptor in mediating the inhibitory activity of myelin inhibitors. *Neuron* **45**, 345–351
3. Shao, Z., Browning, J. L., Lee, X., Scott, M. L., Shulga-Morskaya, S., Allaire, N., Thill, G., Levesque, M., Sah, D., McCoy, J. M., Murray, B., Jung, V., Pepinsky, R. B., and Mi, S. (2005) TAJ/TROY, an orphan TNF receptor family member, binds Nogo-66 receptor 1 and regulates axonal regeneration. *Neuron* **45**, 353–359
4. Mi, S. (2008) Troy/Taj and its role in CNS axon regeneration. *Cytokine Growth Factor Rev.* **19**, 245–251
5. Schwab, M. E. (2010) Functions of Nogo proteins and their receptors in the nervous system. *Nat. Rev. Neurosci.* **11**, 799–811
6. McDonald, C. L., Bandtlow, C., and Reindl, M. (2011) Targeting the Nogo receptor complex in diseases of the central nervous system. *Curr. Med. Chem.* **18**, 234–244
7. Mandemakers, W. J., and Barres, B. A. (2005) Axon regeneration. It's getting crowded at the gates of TROY. *Curr. Biol.* **15**, R302–305
8. Bodmer, J. L., Schneider, P., and Tschopp, J. (2002) The molecular architecture of the TNF superfamily. *Trends Biochem. Sci.* **27**, 19–26
9. Kojima, T., Morikawa, Y., Copeland, N. G., Gilbert, D. J., Jenkins, N. A., Senba, E., and Kitamura, T. (2000) TROY, a newly identified member of the tumor necrosis factor receptor superfamily, exhibits a homology with Edar and is expressed in embryonic skin and hair follicles. *J. Biol. Chem.* **275**, 20742–20747
10. Eby, M. T., Jasmin, A., Kumar, A., Sharma, K., and Chaudhary, P. M. (2000) TAJ, a novel member of the tumor necrosis factor receptor family, activates the c-Jun N-terminal kinase pathway and mediates caspase-independent cell death. *J. Biol. Chem.* **275**, 15336–15342
11. Wang, Y., Li, X., Wang, L., Ding, P., Zhang, Y., Han, W., and Ma, D. (2004) An alternative form of paraptosis-like cell death, triggered by TAJ/TROY and enhanced by PDCD5 overexpression. *J. Cell Sci.* **117**, 1525–1532
12. Schwab, J. M., Tuli, S. K., and Failli, V. (2006) The Nogo receptor complex. Confining molecules to molecular mechanisms. *Trends Mol. Med.* **12**, 293–297
13. Yamashita, T., and Tohyama, M. (2003) The p75 receptor acts as a displacement factor that releases Rho from Rho-GDI. *Nat. Neurosci.* **6**, 461–467
14. Garcia-Mata, R., Boulter, E., and Burridge, K. (2011) The "invisible hand." Regulation of RHO GTPases by RHOGDIs. *Nat. Rev. Mol. Cell Biol.* **12**, 493–504
15. Lee, K. F., Li, E., Huber, L. J., Landis, S. C., Sharpe, A. H., Chao, M. V., and Jaenisch, R. (1992) Targeted mutation of the gene encoding the low affinity NGF receptor p75 leads to deficits in the peripheral sensory nervous system. *Cell* **69**, 737–749
16. Zhang, Y., Yan, Z., Farooq, A., Liu, X., Lu, C., Zhou, M. M., and He, C. (2004) Molecular basis of distinct interactions between Dok1 PTB domain and tyrosine-phosphorylated EGF receptor. *J. Mol. Biol.* **343**, 1147–1155
17. Liu, X., Wang, Y., Zhang, Y., Zhu, W., Xu, X., Niinobe, M., Yoshikawa, K., Lu, C., and He, C. (2009) Nogo-A inhibits necdin-accelerated neurite outgrowth by retaining necdin in the cytoplasm. *Mol. Cell. Neurosci.* **41**, 51–61
18. Zhang, Y., Wang, Y. G., Zhang, Q., Liu, X. J., Liu, X., Jiao, L., Zhu, W., Zhang, Z. H., Zhao, X. L., and He, C. (2009) Interaction of Mint2 with TrkA is involved in regulation of nerve growth factor-induced neurite outgrowth. *J. Biol. Chem.* **284**, 12469–12479
19. Hatten, M. E. (1985) Neuronal regulation of astroglial morphology and proliferation *in vitro*. *J. Cell Biol.* **100**, 384–396
20. Jiao, L., Zhang, Y., Hu, C., Wang, Y. G., Huang, A., and He, C. (2011) Rap1GAP interacts with RET and suppresses GDNF-induced neurite outgrowth. *Cell Res.* **21**, 327–337
21. Su, Z., Cao, L., Zhu, Y., Liu, X., Huang, Z., Huang, A., and He, C. (2007) Nogo enhances the adhesion of olfactory ensheathing cells and inhibits their migration. *J. Cell Sci.* **120**, 1877–1887
22. Ren, X. D., Kiosses, W. B., and Schwartz, M. A. (1999) Regulation of the small GTP-binding protein Rho by cell adhesion and the cytoskeleton. *EMBO J.* **18**, 578–585
23. Liu, X., Lu, Y., Zhang, Y., Li, Y., Zhou, J., Yuan, Y., Gao, X., Su, Z., and He, C. (2012) Slit2 regulates the dispersal of oligodendrocyte precursor cells via Fyn/RhoA signaling. *J. Biol. Chem.* **287**, 17503–17516
24. Wang, K. C., Kim, J. A., Sivasankaran, R., Segal, R., and He, Z. (2002) P75 interacts with the Nogo receptor as a co-receptor for Nogo, MAG and

OMgp. *Nature* **420**, 74–78
25. Zhang, Y., Zhu, W., Wang, Y. G., Liu, X. J., Jiao, L., Liu, X., Zhang, Z. H., Lu, C. L., and He, C. (2006) Interaction of SH2-Bβ with RET is involved in signaling of GDNF-induced neurite outgrowth. *J. Cell Sci.* **119**, 1666–1676
26. Harrington, A. W., Li, Q. M., Tep, C., Park, J. B., He, Z., and Yoon, S. O. (2008) The role of Kalirin9 in p75/nogo receptor-mediated RhoA activation in cerebellar granule neurons. *J. Biol. Chem.* **283**, 24690–24697
27. Michaelson, D., Silletti, J., Murphy, G., D'Eustachio, P., Rush, M., and Philips, M. R. (2001) Differential localization of Rho GTPases in live cells. Regulation by hypervariable regions and RhoGDI binding. *J. Cell Biol.* **152**, 111–126
28. Samuel, F., and Hynds, D. L. (2010) RHO GTPase signaling for axon extension. Is prenylation important? *Mol. Neurobiol.* **42**, 133–142
29. Morikawa, Y., Hisaoka, T., Kitamura, T., and Senba, E. (2008) TROY, a novel member of the tumor necrosis factor receptor superfamily in the central nervous system. *Ann. N.Y. Acad. Sci.* **1126**, A1–A10
30. Etienne-Manneville, S., and Hall, A. (2002) Rho GTPases in cell biology. *Nature* **420**, 629–635
31. Hall, A. (1998) Rho GTPases and the actin cytoskeleton. *Science* **279**, 509–514
32. Luo, L. (2000) Rho GTPases in neuronal morphogenesis. *Nat. Rev. Neurosci.* **1**, 173–180
33. Gorovoy, M., Neamu, R., Niu, J., Vogel, S., Predescu, D., Miyoshi, J., Takai, Y., Kini, V., Mehta, D., Malik, A. B., and Voyno-Yasenetskaya, T. (2007) RhoGDI-1 modulation of the activity of monomeric RhoGTPase RhoA regulates endothelial barrier function in mouse lungs. *Circ. Res.* **101**, 50–58
34. Boulter, E., and Garcia-Mata, R. (2010) RhoGDI. A rheostat for the Rho switch. *Small GTPases* **1**, 65–68
35. McMahon, S. B., Armanini, M. P., Ling, L. H., and Phillips, H. S. (1994) Expression and coexpression of Trk receptors in subpopulations of adult primary sensory neurons projecting to identified peripheral targets. *Neuron* **12**, 1161–1171
36. Yamashita, T., Higuchi, H., and Tohyama, M. (2002) The p75 receptor transduces the signal from myelin-associated glycoprotein to Rho. *J. Cell Biol.* **157**, 565–570
37. Wright, D. E., and Snider, W. D. (1995) Neurotrophin receptor mRNA expression defines distinct populations of neurons in rat dorsal root ganglia. *J. Comp. Neurol.* **351**, 329–338
38. Hisaoka, T., Morikawa, Y., Komori, T., Sugiyama, T., Kitamura, T., and Senba, E. (2006) Characterization of TROY-expressing cells in the developing and postnatal CNS. The possible role in neuronal and glial cell development. *Eur. J. Neurosci.* **23**, 3149–3160
39. Hisaoka, T., Morikawa, Y., and Senba, E. (2006) Characterization of TROY/TNFRSF19/TAJ-expressing cells in the adult mouse forebrain. *Brain Res.* **1110**, 81–94
40. Mi, S., Lee, X., Shao, Z., Thill, G., Ji, B., Relton, J., Levesque, M., Allaire, N., Perrin, S., Sands, B., Crowell, T., Cate, R. L., McCoy, J. M., and Pepinsky, R. B. (2004) LINGO-1 is a component of the Nogo-66 receptor/p75 signaling complex. *Nat. Neurosci.* **7**, 221–228
41. Chumbalkar, V. C., Subhashini, C., Dhople, V. M., Sundaram, C. S., Jagannadham, M. V., Kumar, K. N., Srinivas, P. N., Mythili, R., Rao, M. K., Kulkarni, M. J., Hegde, S., Hegde, A. S., Samual, C., Santosh, V., Singh, L., and Sirdeshmukh, R. (2005) Differential protein expression in human gliomas and molecular insights. *Proteomics* **5**, 1167–1177
42. Cordle, A., Koenigsknecht-Talboo, J., Wilkinson, B., Limpert, A., and Landreth, G. (2005) Mechanisms of statin-mediated inhibition of small G-protein function. *J. Biol. Chem.* **280**, 34202–34209
43. Boulter, E., Garcia-Mata, R., Guilluy, C., Dubash, A., Rossi, G., Brennwald, P. J., and Burridge, K. (2010) Regulation of Rho GTPase crosstalk, degradation and activity by RhoGDI1. *Nat. Cell Biol.* **12**, 477–483
44. Paulino, V. M., Yang, Z., Kloss, J., Ennis, M. J., Armstrong, B. A., Loftus, J. C., and Tran, N. L. (2010) TROY (TNFRSF19) is overexpressed in advanced glial tumors and promotes glioblastoma cell invasion via Pyk2-Rac1 signaling. *Mol. Cancer Res.* **8**, 1558–1567
45. Jacobs, V. L., Liu, Y., and De Leo, J. A. (2012) Propentofylline targets TROY, a novel microglial signaling pathway. *PLoS ONE* **7**, e37955
46. Deighton, R. F., McGregor, R., Kemp, J., McCulloch, J., and Whittle, I. R. (2010) Glioma pathophysiology. Insights emerging from proteomics. *Brain Pathol.* **20**, 691–703
47. Li, X., Law, J. W., and Lee, A. Y. (2012) Semaphorin 5A and plexin-B3 regulate human glioma cell motility and morphology through Rac1 and the actin cytoskeleton. *Oncogene* **31**, 595–610
48. Johnston, A. L., Lun, X., Rahn, J. J., Liacini, A., Wang, L., Hamilton, M. G., Parney, I. F., Hempstead, B. L., Robbins, S. M., Forsyth, P. A., and Senger, D. L. (2007) The p75 neurotrophin receptor is a central regulator of glioma invasion. *PLoS Biol.* **5**, e212
49. Shimizu, A., Mammoto, A., Italiano, J. E., Jr., Pravda, E., Dudley, A. C., Ingber, D. E., and Klagsbrun, M. (2008) ABL2/ARG tyrosine kinase mediates SEMA3F-induced RhoA inactivation and cytoskeleton collapse in human glioma cells. *J. Biol. Chem.* **283**, 27230–27238